# SIMULATION OF AVALANCHES IN CAMPUS LICENSE OF ANSYS FLUENT

Jan Pala[1, 2]*, Ales Palkovic[1], and Jiri Teichman[1]

[1] *TechSoft Engineering, spol. s r.o. Prague, Czech Republic*
[2] *Third Medical Faculty Charles University in Prague, Czech Republic*

ABSTRACT: Snow avalanche dynamics is a phenomenon widely studied worldwide. Modelling of avalanche dynamics require several conditions: 1. appropriate software, 2. digital terrain model, 3. photography or local measurement of snow properties in the area of interest, 4. weather and snow forecast to evaluate snow deposition in the terrain, 5. entry and boundary conditions. There are several dedicated software for snow crack propagation, snow avalanche dynamics, etc. Most of these software are not available as freeware and their full and educational licenses are quite expensive for personal, research or educational use. On the other hand, there are general simulation software packages covering multiphysics that are available as academic campus licenses with tens of licenses per individual physics. These academic campus licenses are widely spread for academic purposes at universities and research institutes. Thus, many undergraduate, graduate and Ph.D. students have access to the enterprise versions of Computer Fluid Dynamics (CFD) software. The fifth generation of Digital Terrain Model (DTM 5G) representing natural and human modelled terrain in a form of discrete points is currently available in many countries. As the total mean error of the height in DTM 5G is 0.18 m in an open terrain and 0.3 m in a forested terrain, it could be used for modelling snow layers and avalanche dynamics without additional unmanned aerial vehicle (UAV) Light Detection And Ranging (LiDAR) or satellite data. In our contribution we focus on the application of campus license of CFD solver *Ansys Fluent* for modelling avalanche dynamics in typical avalanche paths in the mountains with comparison with real avalanches.

KEYWORDS: avalanche, terrain, CFD, Ansys Fluent.

## 1. INTRODUCTION

Simulation of snow avalanche release, fatigue and crack propagation in snow, snow dynamic, transport and avalanche debris play important role in many areas of human activities and beings starting from prediction and protection of transport construction such as highways, roads and railways via buildings and populated areas, and culminating in leisure activities in the snow-covered winter terrain such as resort skiing, backcountry skiing, freeride, snowshoeing, winter mountaineering and ice-climbing. Critical safety issue in all these activities is avalanche safety and forecast. Development in computers, graphic card and software in the last few decades enable simulation of snow avalanches of different sizes from small ones up to extreme ones. There are many solvers and software handling dynamic behavior of different phenomena such as dedicated ones, standard is RAMMS developed by SLF (Schnee- und Lawinenforschung) Davos (RAMMS, 2024), and general CFD in 2D or 3D such as *Ansys Fluent*. There were introduced many other approaches to study snow dynamics during avalanche release and transportation with some advantages and limitations in comparison with other approaches. One of them nicely covering not only avalanches themselves, but also interaction between avalanches and obstacles, forests or lakes is Depth Averaged Material Point Method (DAMPM), Gaume, J. (2023). The goal of this contribution is to propose a methodology for avalanche simulation in 3D environment based on real terrain data. Academic license of commercial CFD solver *Ansys Fluent* will be used as it is available to many universities and research institutions. Due to *Ansys Fluent* being general purpose CFD modelling tool, the methodology and capabilities of the simulation proposed in this article can easily be further expanded (e. g. adding obstacles to the avalanche path, human triggering, tuning snow material properties, etc.).

## 2. REFERENCE AVALANCHE

Our aim is to show workflow that could be used by anybody with the access to appropriate terrain data and avalanche measurements for the comparison of simulations with the reality. Standard avalanche cadastres in the Czech Republic are known only in the two highest mountain ranges - Krkonoše and Jeseníky. While avalanches occur only exceptionally in the Jeseníky, they are relatively frequent in the Krkonoše. Thus, as a reference example we choose the biggest known avalanche that was self-triggered in the Modrý Důl (Blue Valley) located in Krkonoše National Park on the border between the Czech Republic and Poland in February 10, 2015.

* *Corresponding author address:*
Jan Pala, TechSoft Engineering, spol. s .r.o., Milevská 209/5, 140 00 Praha 4, Czech Republic;
tel: +420 770 168 110;
email: pala@techsoft-eng.cz

Figure 1: The slope after avalanche fall photographed by Kořízek, V. (2015), Racek, O. (2015).

The avalanche cadastre in Krkonoše is studied in detail since 1961, and there were recorded 16 avalanches in this avalanche path till 2015 (Figure 1). Of these sixteen, fourteen were spontaneously triggered and two were artificially triggered. The width of the crown was measured in the range from 40 to 210 m, height of the crown in the range from 0.3 to 3 m, length of the avalanche path from 100 up to 600 m and the height of avalanche debris varied from 0.7 to 3 m. The spontaneously triggered avalanche at the avalanche danger level three in February 10, 2015 was significantly bigger with the width of the crown 550 m, height of the crown 0.35-2.40 m (average 1.07 m), length of avalanche path 1 100 m, and the area of the avalanche 154 740 m$^2$. The avalanche missed the hut *Děvín* by 35 meters thanks to the forest. Some branches and remains of trees ended up on the roof of the hut The height of avalanche debris was not measured (Kořízek, V. (2015), Racek, O. (2015), Tryzna, V. (2015)).

## 3. 3D TERRAIN DATA

Based on the avalanche data provided by Kořízek, V. (2015) and Tryzna, V. (2015), the region encapsulating the area of interest was selected (Figure 2).

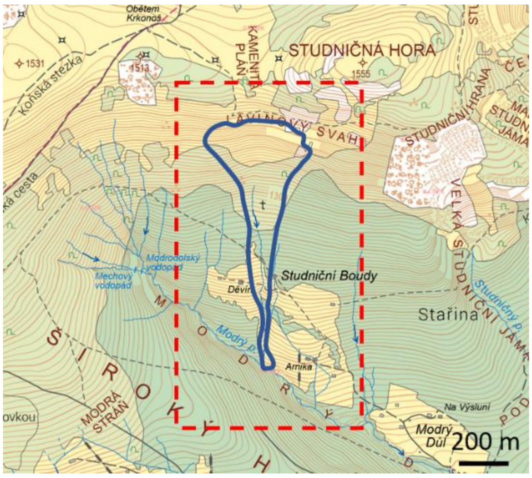


Figure 2: Area selected for the simulation (depicted by the red dashed line) by State Administration of Land Surveying and Cadastre, 2024. Avalanche area depicted by blue line.

The area has dimensions of 1.5 x 0.9 km with the elevation ranging from 1 010 m to 1 558 m above sea level. The selected area was then exported as XYZ data points to be used as a basis for the 3D computational mesh (Figure 3). These data points were based on the DTM 5G model.

The XYZ raw data were processed and converted to the STL file (file format for description of a raw, unstructured triangulated surface) in the free software tool *MeshLab*. Firstly, the normal of the point cloud were computed, then continuous surface was reconstructed using Poisson algorithm. The resulting STL surface is depicted in Figure 4.

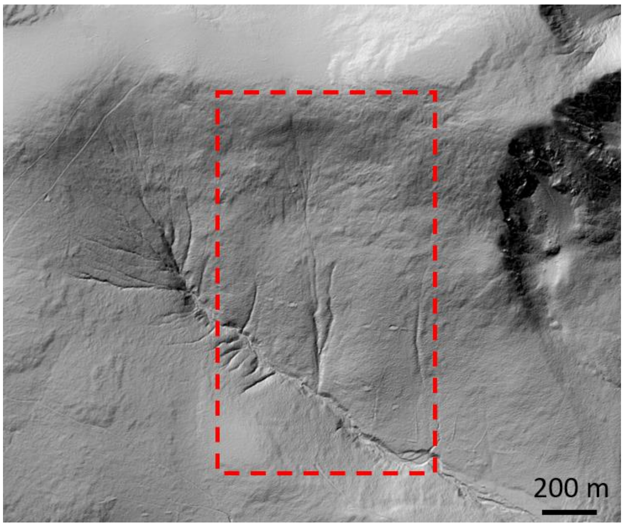


Figure 3: 3D ground surface based on *ZABAGED* DTM 5G data (simulation area depicted by the red dashed line) by ZABAGED (2024).

Figure 4: STL surface extracted from the XYZ point cloud.

Lastly, the forest contour line was manually extracted as a polygonal curve in *Ansys SpaceClaim* to be used in the simulation (Figure 5).

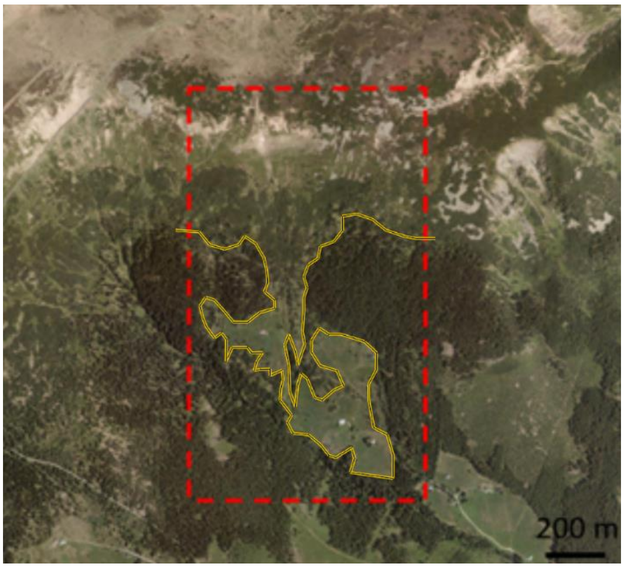


Figure 5: Forested area before the avalanche, orthographic photo from 2014. Simulation area depicted by the red dashed line. Forest contour depicted by yellow line.

## 4. METHODS

In this paper, the avalanche is considered to be continuous phase material, so the finite volume method was utilized.

### *4.1 Snow Properties and Dynamics*

In general, snow behavior as a continuum is governed by two phenomena. In the bulk flow by density and dynamic viscosity. And by the contact behavior of the snow-ground surface contact, which is controlled by the surface zone boundary condition.

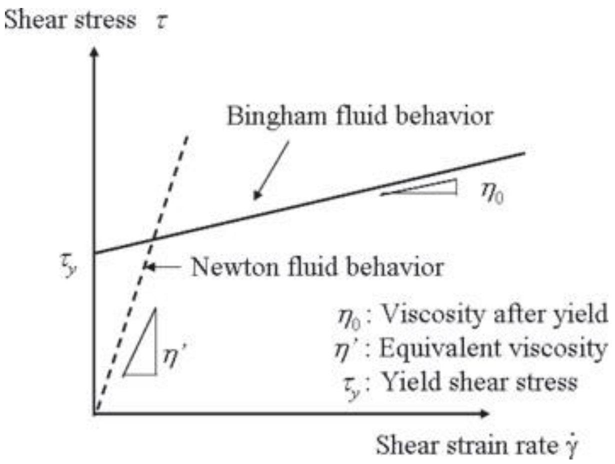


Figure 6: Schematic relationship between a Bingham fluid shear strain rate and shear stress, Oda, K. (2011). The difference of the Bingham fluid behavior compared to Newtonian fluid is that yield shear stress threshold must be reached before the material is being fluidized.

The avalanche is assumed to be homogenous, isotropic and incompressible. These assumptions are not unreasonable considering other simplifications showed (e. g. Bingham viscosity model) by Whipple, K. X. (1997).

Snow can be described as a Bingham fluid in regards of its viscosity described by Whipple, K. X. (1997) Oda, K. (2011) and Aggarwal, R.K. (2013). The Bingham fluid behavior is shown in Figure 6.

In general, shear stress $\tau$ in Bingham fluid can be defined by equation (1).

$$\tau = \mu_0 \dot{\gamma} + \tau_y \qquad (1)$$

where $\mu_0$ is the dynamic viscosity after yield, $\dot{\gamma}$ is the shear strain rate and $\tau_y$ is the yield shear strength. The yield shear strength for snow, in general, depends on cohesion $c$, internal friction angle $\theta$ and dynamic pressure $p$ (Oda, K. (2011)). Substituting these values for $\tau_y$ and rearranging equation (1), the dynamic viscosity of snow can be written as (2).

$$\mu = \mu_0 + \frac{c + p\ tan\theta}{\dot{\gamma}} \qquad (2)$$

To avoid singularity when strain rate is zero, the artificial viscosity for non-moving fluid was introduced as $10^5\ Pa \cdot s$ and the final expression for dynamic viscosity was defined as equation (3).

$$\mu = min\left(10^5, \mu_0 + \frac{\tau_y}{\dot{\gamma}}\right) \qquad (3)$$

Assumption was made, that the cohesion, internal friction angle and the dynamic pressure does not individually affect large scale avalanche behavior and that these parameters can be simplified to a constant value, that can be tuned. This assumption is supported by Dent J. D. (1982), Barry Voight, B. (1994) and Birte, D. (2012).

Material properties used in the simulations are summarized in Table 1.

Table 1: Material properties of the snow used in the simulation.

| Parameter | Snow | Air |
|---|---|---|
| Dynamic viscosity (Pa·s) | 2 | $1.7894 \cdot 10^{-5}$ |
| Density (kg·m$^{-3}$) | 500 | 1.225 |
| Yield shear strength (Pa) | 1 0 0 0 | - |

### *4.2 Numerical Method*

For capturing avalanche spatial propagation, unsteady pressure based laminar solver with Volume of Fluid (VOF) model was used in *Ansys Fluent 2024 R2*. This model solves continuum and momentum equation for the whole pressure and velocity field and calculates volume fraction of the secondary phase $q$ using continuity equation for the volume fraction (4):

$$\frac{1}{\rho_q}\left[\frac{\partial}{\partial t}\left(\alpha_q\rho_q\right) + \nabla\cdot\left(\alpha_q\rho_q\overrightarrow{v_q}\right)\right] = 0 \qquad (4)$$

where $\rho$ is the density, $\alpha$ is the volume fraction and $v$ is the velocity. The volume fraction of the primary phase is then computed by the equation (5):

$$\sum_{q=1}^{n}\alpha_q = 1 \qquad (5)$$

The solver time advancement was controlled using adaptive time step size based on the simulation global Courant number (CFL). The settings of the solver are summarized in Table 2.

Table 2: Solver settings.

| Setting | Value |
|---|---|
| CFL | 2 |
| Scheme | SIMPLE |
| VOF formulation | Explicit |
| Pressure discretization | PRESTO! |
| Momentum discretization | Second order |
| Volume Fraction | Geo-Reconstruct |
| Transient formulation | First order implicit |
| Gravitational acceleration ($m{\cdot}s^{-2}$) | -9.81 |

## *4.3 Computational Mesh*

The computational mesh was based on the STL surface generated from the XYZ point cloud (Figure 4). The STL file was remeshed in *Ansys Fluent 2024 R2* with constant surface cell size of 6 m, which maintains all important topographical features. This value is large enough to capture major terrain features and is not prohibitively fine. The resulting surface mesh is depicted in Figure 7.

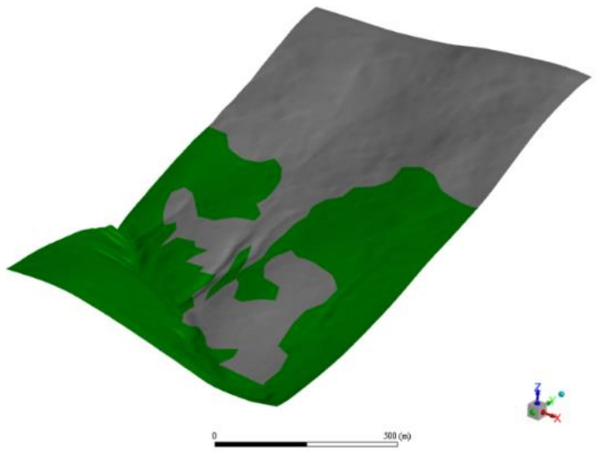


Figure 7: Bottom surface (surface representing ground) of the computational mesh used. Green color depicts forested area.

The surface mesh was then extruded in normal direction with initial layer height of 0.05 m, 22 total number of layers, 1.2 growth rate and total height of 13.5 m. The resulting computational mesh had total size of 1 183 644 cells. The cross-section of the mesh is depicted in Figure 8 and the terrain height in Figure 8.

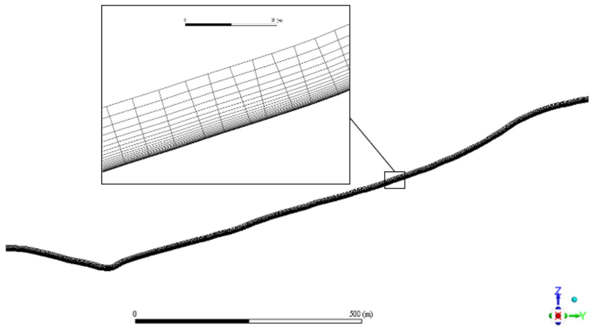

Figure 8: Cross-section of the computational mesh in the middle of the domain. The whole slope profile and the riverbed can be seen. The mesh is conformally sized across the whole domain. In the detail the normal height of the mesh can be seen as well as sizing of the cells.

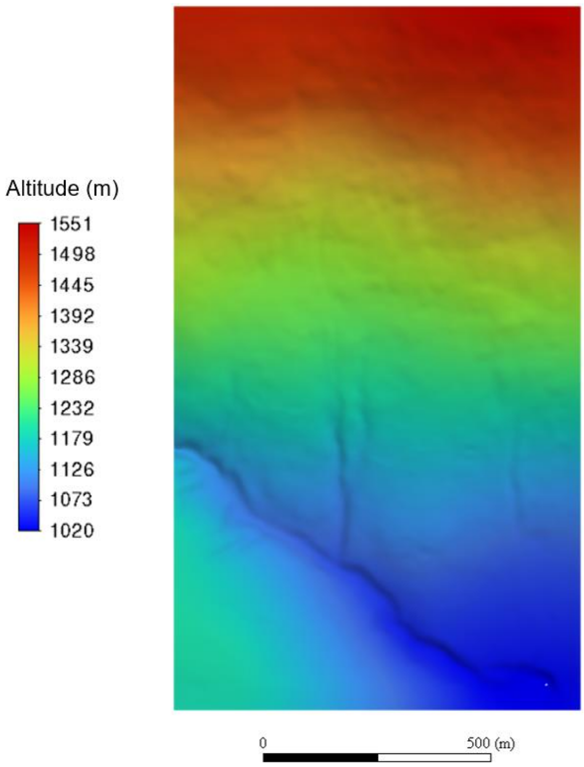


Figure 9: Contours of altitude (z-coordinate) of the simulated area. The contours show little to no altitude change in avalanche transversal direction. This implies no guiding for the avalanche movement and thus the shape will be mostly affected by terrain type (smooth, forest, etc.).

## *4.4 Boundary Conditions*

For the bottom surface of the domain (snow-covered surface), the shear stress was defined as $0Pa$ (free slip condition) to allow for the avalanche movement as it is a high viscous fluid. The forested surface was set as a no-slip wall to slow-down the avalanche progress. Side walls and upper surface of the domain were set as a symmetry boundary condition (zero-shear slip wall). The boundary conditions used are summarized in Table 3.

Table 3: Boundary conditions. All boundary conditions are of type wall.

| Zone | Condition |
|---|---|
| Ground surface | Free slip |
| Forested surface | No slip |
| Top and side domain walls | Free slip |

### 4.5 *Initial Conditions and Release Area*

The simulation is initialized with zero velocities and zero gauge pressure. The snow phase volumetric fraction is patched to the volume depicted in Fig. 9. The height of the snow fraction measured normal to the surface is assumed to be constant with value of 1.4 m, which is higher than average of the avalanche crown height measured by Kořízek, V. (2015) and Tryzna, V. (2015) but better represents the height of the central section of the avalanche.

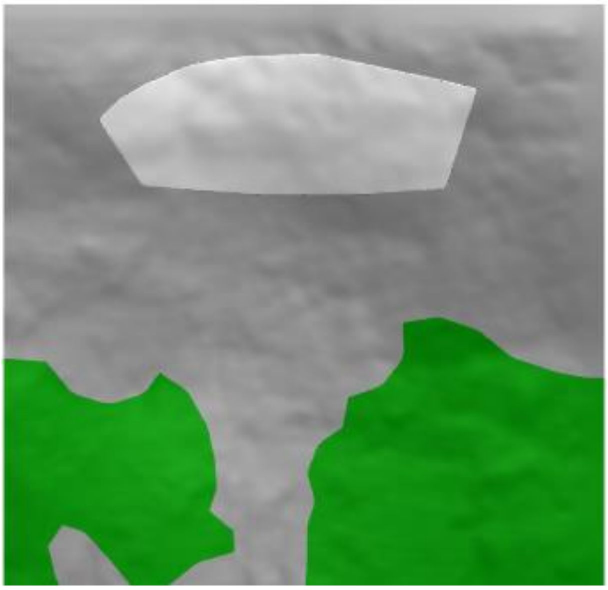

Figure 10: The release area of the avalanche viewed from top. The snow volume fraction is depicted by the white color. Only upper part of the computational domain is shown.

The definitions of release areas and release heights have a very strong impact on the results of the simulations, this should be done by people with experience concerning the topographic and meteorological situation of the investigation area, RAMMS (2024).

### 4.6 *Avalanche Energy Dissipation and Breakup*

As continuum approach was used, breakup of the avalanche was not modeled explicitly as well as energy equation was not used in the simulation. To stop the avalanche, some authors propose incremental viscosity increase, Voight, B. (1994) or no-slip boundary condition at the bottom of the slope, Aggarwal, R. K. (2013). In this paper, to account for the energy loss and breakup of the avalanche, momentum sink $S$ was introduced in the liquid phase. The momentum sink was defined for all directions by the equation (6):

$$S_i = -\frac{v_i \rho f_d}{\Delta t} \qquad (6)$$

where $v_i$ is the velocity component in $i$ direction $\rho$ is the density $f_d$ is the dissipation function and $\Delta t$ is the time interval of the force application which is $1\,s$. The dissipation function is defined by (7):

$$f_d = max(Ay + B, 0) \qquad (7)$$

where $A$ and $B$ are model constants and $y$ is the coordinate in the direction the avalanche traveled. In this simulation, the $A$ and $B$ coefficients are set to $-0.001\,m^{-1}$ and $0.5$ respectively. In the forested area, these coefficients were set to $0\,m^{-1}$ for $A$ and $0.01$ for $B$.

## 5 RESULTS AND DISCUSSION

The simulation was run until the avalanche reached the *Modrý potok* riverbed, which took approximately 40 seconds. The shape and height of the avalanche in six different time points is shown in Figure 11, where we have applied approximation and simplification in the definition of the crown of the avalanche with the constant height over the release width.

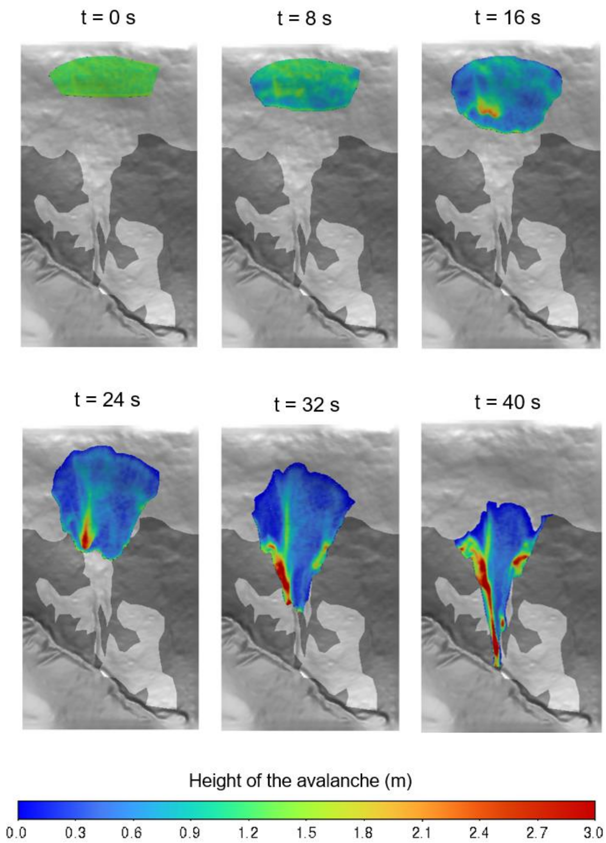

Figure 11: Contours of avalanche height evaluated as a boundary normal distance from the terrain surface to the iso-surface of 0.5 volume fraction of snow.

The simulation in campus academic version of *Ansys Fluent* shows the development of the avalanche of the initial open part of the slope with subsequent channeling through the matured forest into a narrowing terrain depression as shown by the DTM 5G data in Figure 2. We only considered the movement of the snow mass in the simulation and did not consider the air flow accompanying the snow mass movement that destroy partially the forest in the avalanche path and *Modrý potok* riverbed.

The simulation results show good agreement of the overall avalanche shape with the in-situ measurement performed by Kořízek, V. (2015) and Tryzna, V. (2015). The simulation shows expected accumulation of snow near the edge of the forest and at the riverbed. The time accuracy of the simulation can't be confirmed as no direct observation of the avalanche fall is available, however its speed shows good agreement with data obtained by Havens, S (2014).

## 6 CONCLUSION

We show possible application of general CFD solver *Ansys Fluent* available among academic campus licenses for modelling snow avalanches. The biggest avalanche released in the known time in the Czech Republic on Feb 10, 2015, was modeled based on DTM 5G, forested terrain before the avalanche and the terrain measurement after avalanche. We focused on general practical workflow for simulation of snow avalanches that can be employed in any area where appropriate DTM 5G terrain model is available as the source of precise entry data for simulation.

The model proposed can further be improved by introducing variable yield shear strength of the snow, partial slip condition for the different terrain types and by improving the definition of the dissipation function which is now based only on distance travelled and not on any physical quantity. Other improvement could employ more detailed definition of obstacles as trees and rocks on the slope influencing speed, direction and accumulation of the snow via avalanche path, and human influence of avalanche release.

## ACKNOWLEDGEMENT

We acknowledge TechSoft Engineering, spol. s r.o. for the support for this contribution.

## REFERENCES

Ansys, Fluent 2024 R2 Theory Guide, Canonsburg, 2024.

Ansys, Fluent 2024 R2 User's Guide, Canonsburg, 2024.

Aggarwal, R. K., Kumar, A., Application of CFD code for simulation of an inclined snow chute flow, 2013.

Birte, D., Shiva, P. P., Full two-dimensional rapid chute flows of simple viscoplastic granular materials with a pressure-dependent dynamic slip-velocity and their numerical simulations, Journal of Non-Newtonian Fluid Mechanics, Volumes 173–174, 2012.

Dent, J. D., Lang, T. E., Experiments on mechanics of flowing snow, Cold Regions Science and Technology, Volume 5, Issue 3, 1982, Pages 253-258, ISSN 0165-232X, 1982.

Gaume, J., Recent Advances in Modeling Snow and Avalanches with the Material Point Method and Practical Implications, ISSW 2023, Bend, Oregon.

Kořízek, V., Avalanche in Modrý Důl, Alpy4000.cz, 2015.

Oda, K., et al., Simulation of a snow avalanche model test using computational fluid dynamics, 2011.

Orthophoto, 2014.

Racek, O., Snow avalanche modelling, BSc. thesis, Charles University in Prague, Czech Republic, 2015.

RAMMS_AVAL_Manual, 2024.

Scott, H., et al., Calculating the velocity of a fast-moving snow avalanche using an infrasound array, 2014.

State Administration of Land Surveying and Cadastre, 2024.

Tryzna, V., Distribution of snow in the eastern Giant mountains in the winter 2014/2015; conference HYDROMODE 2015, Kostelec nad Cernymi lesy, Czech Republic, 14. - 15. 9. 2015.

Voight, B., Sousa, J., Lessons from Ontake-san: A comparative analysis of debris avalanche dynamics, Engineering Geology, Volume 38, Issues 3–4, Pages 261-297, ISSN 0013-7952, 1994.

Whipple, K. X., Open-Channel Flow of Bingham Fluids: Applications in Debris-Flow Research. The Journal of Geology 105, no. 2, 243–62, 1997.

ZABAGED, https://ags.cuzk.cz/geoprohlizec/.